ChemComm

COMMUNICATION

View Article Online
View Journal | View Issue

Cite this: *Chem. Commun.*, 2014, **50**, 4607

Received 28th January 2014,
Accepted 10th March 2014

DOI: 10.1039/c4cc00758a

www.rsc.org/chemcomm

Ligand tuning of single-site manganese-based catalytic antioxidants with dual superoxide dismutase and catalase activity†

Michaela Grau,[a] Francesco Rigodanza,[b] Andrew J. P. White,[a] Antonio Sorarù,[b] Mauro Carraro,[b] Marcella Bonchio*[b] and George J. P. Britovsek*[a]

A bio-inspired manganese(II) complex with a linear pentadentate ligand framework containing soft sulfur donors and an alternating NSNSN binding motif displays excellent dual CAT/SOD-like antioxidant activity with high turnover efficiency and good operation stability in an aqueous environment.

As a by-product of respiration, oxidative stress in living systems is a major source of irreversible cell damage and severe pathologies. Failure of the four electron O_2 reduction chain can give rise to an unbalanced build-up of so called Reactive Oxygen Species (ROS), namely the superoxide radical ($O_2^{\cdot-}$) and hydrogen peroxide (H_2O_2). These powerful oxidants can attack tissues, membranes and their proteic environment, thereby turning into lethal agents against cell structure and functioning. *In vivo* protection occurs *via* suppression of the ROS cytotoxins through a cascade of dismutation processes. These reactions are mediated by two key classes of metallo-enzymes: superoxide dismutases (SODs) and catalases (CATs), both of which exist as manganese forms.[1,2]

Mn(SOD)s are oxidoreductases with a mononuclear active site that cycles between the reduced Mn(II) and the oxidised Mn(III) state, whereas Mn(CAT)s contain a dinuclear Mn core with bridging carboxylate and oxide ligands (Scheme 1).[3] A cooperative antioxidant effect against ROS injury stems from cascade reactions of SOD-mediated conversion of the superoxide radical to oxygen and hydrogen peroxide, followed by decomposition of hydrogen peroxide to water and oxygen by CAT.

Recent efforts have been dedicated to the discovery of novel synthetic single-site Mn complexes with both SOD and CAT activity that can be used as artificial small molecule catalysts for ROS detoxification, following bio-inspired guidelines. Indeed, some

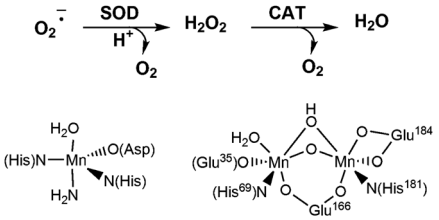

Scheme 1 Cooperative SOD/CAT actions for ROS detoxification by manganese-based enzymes.

Mn(III)–porphyrin and –salen complexes (for example AEOL10150 and EUK-134) as well as seven-coordinate Mn(II) complexes with macrocyclic aza-ligands (M40403) have entered clinical trials as synthetic catalytic antioxidants (Fig. 1).[4–8] In particular the M40403 aza-complex has outperformed the rate of the native Mn(SOD) enzyme, but fails to exhibit dual SOD and CAT activity, which has been reported for certain porphyrin and salen complexes.

We present here our studies on a series of seven-coordinate Mn(II) complexes with linear pentadentate ligands **1–3** (Fig. 1) and their potential as catalytic antioxidants by evaluating their

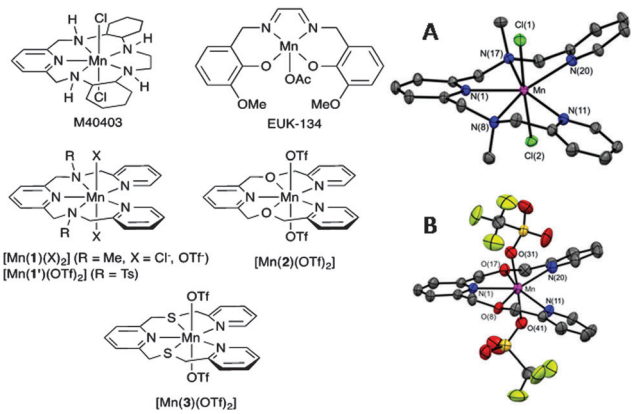

Fig. 1 Seven-coordinate Mn(II) complexes containing linear pentadentate ligands with N, O and S donors (**1–3**) and the structures of the related SOD mimics M40403 and EUK-134. Molecular structure of (A) [Mn(**1**)Cl_2] and (B) [Mn(**2**)$(OTf)_2$] (50% probability ellipsoids).

[a] *Department of Chemistry, Imperial College London, Exhibition Road, South Kensington, London SW7 2AY, UK. E-mail: g.britovsek@imperial.ac.uk*
[b] *ITM-CNR and Department of Chemical Sciences, University of Padova, via Marzolo 1, 35131 Padova, Italy. E-mail: marcella.bonchio@unipd.it*

† Electronic supplementary information (ESI) available: Synthesis and characterisation of ligands and complexes, and details of spectroscopic and X-ray analysis. CCDC 958982 and 958983. For ESI and crystallographic data in CIF or other electronic format see DOI: 10.1039/c4cc00758a

activity as CAT and SOD mimics. The series comprises isostructural ligands with both hard nitrogen and oxygen donors (NMe)2Py3 (**1**), (NTs)2Py3 (**1′**) and O2Py3 (**2**) as well as a soft sulfur-containing analogue S2Py3 (**3**). In previous observations with a pentadentate SNNNS manganese complex, sulfur donors were found to inhibit antioxidant activity.[10] In contrast, we show herein that the [Mn(**3**)(OTf)$_2$] complex with an alternating NSNSN binding motif shows dual CAT and SOD activity *both in CH_3CN and in aqueous solution*, the highest in the series, surpassing the nitrogen and oxygen-based complexes.

Details regarding the synthesis and characterisation of the ligands and metal complexes are provided in the ESI.† A seven-coordinate geometry is confirmed for complexes [Mn(**1**)Cl$_2$] and [Mn(**2**)(OTf)$_2$] in the solid state (Fig. 1) and which is comparable to the structure of the macrocyclic Mn(II) complex related to M40403.‡[11] In all cases, a distorted pentagonal bipyramidal coordination geometry is observed with a noticeable difference in the bending of the N(1) pyridyl ring plane out of the pentagonal plane. In [Mn(**1**)Cl$_2$] and [Mn(**2**)(OTf)$_2$], the metal lies *ca.* 0.09 and 0.08 Å out of the N(1) pyridyl ring plane, whereas in M40403, the metal lies *ca.* 0.45 Å out of this plane.

Triflate ligands are generally weakly coordinating and are easily displaced in acetonitrile or aqueous solutions to give complexes of the type [Mn(L)(S)$_2$](OTf)$_2$ with coordinated solvent ligands (S = acetonitrile or water) and uncoordinated triflate anions. The Mn(II) complexes studied here are high spin over the temperature range from 233 to 343 K in an acetonitrile solution, with magnetic moment values of 5.9–6.0 μ_B (see Fig. S1, ESI†). NMR spectroscopy is normally not useful for Mn(II) complexes due to the extreme line-broadening caused by the paramagnetic Mn(II) centre. However, the ^{19}F NMR spectra for [Mn(**1**)(OTf)$_2$] in CD_3CN over the temperature range from 233 and 343 K do show a broad signal at approximately −70 ppm, which can be assigned to non-coordinating triflate anions and this supports that this complex exists as [Mn(**1**)$(CD_3CN)_2]^{2+}$ in a CD_3CN solution (see Fig. S3 and S4, ESI†). No geometrical changes in coordination, as seen in the case of the related iron complex [Fe(**1**)(OTf)$_2$],[12] were observed for any of these manganese complexes, possibly a consequence of the high spin d^5 configuration and the absence of any ligand field stabilisation. Cyclic voltammograms in acetonitrile are featureless between −1.5 V and +1.5 V (*vs.* Ag/$AgNO_3$) (see Fig. S2, ESI†), as noted for related dicationic seven-coordinate Mn(II) complexes.[13,14] All complexes are essentially colourless and the UV-Vis spectra are featureless at wavelengths above 350 nm. Charge transfer and d–d transitions are not expected in the visible region for these Mn(II) complexes and the only absorptions seen are due to π–π* transitions in the region of 260–270 nm for the pyridine donors and at 234 nm for the tosyl moiety in [Mn(**1′**)(OTf)$_2$] (see Fig. S5a and S5b, ESI†).[15]

The catalase-like activity of the title complexes was initially evaluated in aqueous acetonitrile in the presence of excess H_2O_2 (550 equiv.) by monitoring continuous oxygen evolution (see ESI† for details). The observed catalytic performance has been examined by determining the initial rate (R_0), O_2 yield and turnover number (TON, defined as mol of dioxygen evolved per mol of catalyst). The results are provided in Table 1 and compared with literature data on salen-type complexes, which decompose irreversibly in water after several minutes (entry 1 in Table 1).[2,3]

Table 1 CAT-like activity of mononuclear Mn complexes[16]

#	Compound	R_0 [a] (μM min^{-1})	% O_2 yield (μM)	TON
1	Salen-type complexes[b]	260–29	0.7–3.3 (36–167)	4–17
2	[Mn(**2**)(OTf)$_2$][c]	18	6.3 (1038)	17
3	[Mn(**1**)(OTf)$_2$][c]	29	8.7 (1426)	24
4	[Mn(**1**)(Cl)$_2$][c]	5	0.6 (107)	2
5	[Mn(**1′**)(OTf)$_2$][c]	8	2.4 (397)	7
6	[Mn(**3**)(OTf)$_2$][c]	128	14 (2310)	39
7	[Mn(**3**)(OTf)$_2$][d]	317	>99 (16 500)	275
8	[Mn(**3**)(OTf)$_2$][e]	25	>99 (16 500)	275

[a] Initial reaction rate calculated for O_2 evolution (μM per min). [b] [Mn] = 10 μM, [H_2O_2] = 10 mM, 50 mM phosphate buffer (pH 7–8), 3 min, 25 °C (see ref. 2 and 3). [c] [Mn] = 60 μM, [H_2O_2] = 33 mM, CH_3CN, 2 h, 25 °C. [d] Addition of NaOH aq. (10 μL 1 M), CH_3CN, 5 h. [e] [Mn] = 60 μM, [H_2O_2] = 33 mM, 50 mM borate buffer (pH 9.2), addition of 600 μM imidazole, 14 h, 25 °C.

From Table 1, it can be concluded that [Mn(**3**)(OTf)$_2$] is the most active catalyst within this series for H_2O_2 decomposition and the activity appears to be strongly affected by the nature of the ligand, increasing in the order (NTs)2Py3 (**1′**) < O2Py3 (**2**) < (NMe)2Py3 (**1**) < S2Py3 (**3**) for the bis(triflato) complexes, while the dichlorido complex [Mn(**1**)Cl$_2$] is the least active (entries 2–6 in Table 1). In comparison with previously reported results, these complexes display good catalyst stability as oxygen evolution is detected up to 2 hours of reaction (Fig. S6, ESI†). In all cases, the dismutation activities level off after approximately 20 minutes, but no precipitation or colour change is observed at the end of the reaction. FT-IR analysis of the recovered catalysts did not show any substantial change due to complex degradation (Fig. S7, ESI†).[7] The kinetic profiles at different [Mn(**3**)(OTf)$_2$] concentrations show a well-behaved first order dependence within the range of 30–90 μM (Fig. 2 and Table S1, ESI†). This observation is consistent with the involvement of a single-site catalyst in the rate-determining step of the dismutation process.[17]

The progressive addition of water to the acetonitrile solution resulted in a decrease in the activity of [Mn(**3**)(OTf)$_2$] (Fig. S8, ESI†). The water produced during the dismutation reaction may explain the inhibition at longer reaction times seen in Fig. 2. The change in solvent composition (acetonitrile–water) can have a significant effect on pK_a values. Indeed, the pH of the solution

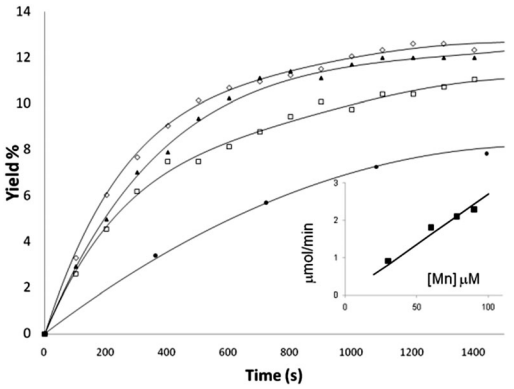

Fig. 2 Yield of oxygen evolution *versus* time at different [Mn(**3**)(OTf)$_2$] concentrations (● 30 μM, □ 60 μM, ▲ 78 μM, ◇ 90 μM) in CH_3CN, 25 °C. Inset: initial rate of O_2 evolution *versus* [Mn(**3**)(OTf)$_2$] concentration.

Table 2 SOD-like activity of mononuclear Mn complexes[16]

Compound	IC_{50} (μM)	k_{McCF} (M^{-1} s^{-1})	Ref.
Thermus thermophilus	n.d.	2×10^9	23
M40403	n.d.	2×10^7	8
EUK-113[a]	0.13–0.7	n.d.	7 and 9
Salen complexes[a]	0.004–0.75	n.d.	9
[Mn(**3**)(OTf)$_2$][b]	0.75	8×10^6	This work
[Mn(**2**)(OTf)$_2$][b]	1.41	4×10^6	This work
[Mn(**1**)(OTf)$_2$][b]	1.51	4×10^6	This work
[Mn(**1**)(Cl)$_2$][b]	2.57	2×10^6	This work
[Mn(**1′**)(OTf)$_2$][b]	Inactive		This work
Ligand **3**[c]	Inactive		This work

[a] Cytochrome 1.0 mM, 1200 units per ml catalase, 50 mM xanthine and sufficient xanthine oxidase to produce a rate of reduction of cytochrome cIII of 0.025 absorbance unit (at 550 nm) per minute. [b] Xanthine 50 μM, NBT 100 μM, xanthine oxidase 0.005 U ml^{-1} in phosphate buffer 50 mM pH 7.4, catalyst 0.6–1.8 μM. [c] Various concentrations: 0.6–1.8 and 6 μM.

appears to have a major influence on the stability of the catalyst system. The addition of small amounts of acid (HCl, 0.1 M, 10 μL) resulted in an immediate loss of CAT activity, whereas the addition of base (NaOH, 1 M, 10 μL) generated a very active (R_0 = 317 μM min^{-1}) and remarkably stable catalyst performance and resulted in quantitative O_2 evolution within 5 hours (entry 7 in Table 1 and Fig. S9, ESI†). Quantitative O_2 evolution was also achieved in *aqueous solution*, using a borate buffer (pH 9) and by the addition of imidazole.[18–20] Under these conditions, a steady oxygen evolution was observed during 14 h with quantitative conversion of H_2O_2 (entry 8, Table 1 and Fig. S10, ESI†).

The novel seven-coordinate Mn(II) complexes of ligands **1–3** also show SOD-like activity in an aqueous environment. The SOD reactivity of all complexes was evaluated using the NBT (nitro blue tetrazolium chloride) method, which allows monitoring of the catalytic removal of O_2^- generated in a xanthine–xanthine oxidase system.[21] SOD activities were determined as IC_{50} (50% inhibition of NBT reduction) and compared on the basis of the kinetic constant (k_{McFC}) when available (Table 2 and ESI†). Overall, the Mn(II) complexes with ligands **1–3** show similar or lower activity compared to the reference complexes EUK-113 and the salen complexes.[7,9,22] Noteworthily, the sulfur-containing complex [Mn(**3**)(OTf)$_2$] provides the highest SOD-like activity within the series with a similar rate constant compared to the benchmark catalyst M40403, which is about two orders of magnitude lower than the natural enzyme.

Mn(II) complexes containing linear pentadentate ligands with an alternating NXNXN binding motif (X = N, O, S) are active single-site catalysts for the dismutation of superoxide and H_2O_2 to oxygen in acetonitrile and, more importantly, *in an aqueous environment*. In particular the sulfur-containing complex [Mn(**3**)(OTf)$_2$] has been found to exhibit high dual SOD/CAT-like activity with excellent catalyst stability in the presence of added base. The sulfur donors in ligand **3** are believed to generate a strong ligand field resulting in increased complex stability under the oxidising testing conditions. Future studies will be directed to identify the key intermediates involved in these dismutation reactions and establish structure–reactivity relationships.

Support from COST Action CM1003 "Biological oxidation reactions – mechanisms and design of new catalysts" is gratefully acknowledged. This work was supported by the Italian MIUR (FIRB, prot. RBAP11ETKA, PRIN "Hi-Phuture" 2010N3T9M4_001) and by Fondazione Cariparo (Nanomode, progetti di eccellenza 2010).

Notes and references

‡ Crystal data for [Mn(**1**)Cl$_2$]: $C_{21}H_{25}Cl_2MnN_5 \cdot CH_2Cl_2$, M = 558.23, orthorhombic, *Pbca* (no. 61), a = 15.97620(17), b = 15.10805(17), c = 21.3826(2) Å, V = 5161.10(9) Å^3, Z = 8, D_c = 1.437 g cm^{-3}, μ(Mo-Kα) = 0.946 mm^{-1}, T = 173 K, colourless blocks, Oxford Diffraction Xcalibur 3S diffractometer; 9061 independent measured reflections (R_{int} = 0.0257), F^2 refinement,[24] R_1(obs) = 0.0349, wR_2(all) = 0.0976, 7581 independent observed absorption-corrected reflections [$|F_o| > 4\sigma(|F_o|)$, $2\theta_{max}$ = 66°], 342 parameters. CCDC 958982. Crystal data for [Mn(**2**)(OTf)$_2$]: $C_{21}H_{19}F_6MnN_3O_8S_2$, M = 674.45, triclinic, $P\bar{1}$ (no. 2), a = 9.9713(3), b = 10.0552(4), c = 14.0070(5) Å, α = 95.426(3), β = 99.237(3), γ = 99.809(3)°, V = 1355.14(9) Å^3, Z = 2, D_c = 1.653 g cm^{-3}, μ(Mo-Kα) = 0.733 mm^{-1}, T = 173 K, colourless tabular needles, Oxford Diffraction Xcalibur 3S diffractometer; 8885 independent measured reflections (R_{int} = 0.0194), F^2 refinement,[24] R_1(obs) = 0.0430, wR_2(all) = 0.1200, 6948 independent observed absorption-corrected reflections [$|F_o| > 4\sigma(|F_o|)$, $2\theta_{max}$ = 66°], 436 parameters. CCDC 958983.

1 S. Miriyala, I. Spasojevic, A. Tovmasyan, D. Salvemini, Z. Vujaskovic, D. St. Clair and I. Batinic-Haberle, *Biochim. Biophys. Acta*, 2012, **1822**, 794–814.
2 A.-F. Miller, *FEBS Lett.*, 2012, **586**, 585–595.
3 S. Signorella and C. Hureau, *Coord. Chem. Rev.*, 2012, **256**, 1229–1245.
4 O. Iranzo, *Bioorg. Chem.*, 2011, **39**, 73–87.
5 D. P. Riley and O. F. Schall, *Adv. Inorg. Chem.*, 2007, **59**, 233–263.
6 G. M. P. Giblin, P. C. Box, I. B. Campbell, A. P. Hancock, S. Roomans, G. I. Mills, C. Molloy, G. E. Tranter, A. L. Walker, S. R. Doctrow, K. Huffman and B. Malfroy, *Bioorg. Med. Chem. Lett.*, 2001, **11**, 1367–1370.
7 S. R. Doctrow, K. Huffman, C. Bucay Marcus, G. Tocco, E. Malfroy, C. A. Adinolfi, H. Kruk, K. Baker, N. Lazarowych, J. Mascarenhas and B. Malfroy, *J. Med. Chem.*, 2002, **45**, 4549–4558.
8 D. Salvemini, Z.-Q. Wang, J. L. Zweier, A. Samouilov, H. Macarthur, T. P. Misko, M. G. Currie, S. Cuzzocrea, J. A. Sikorski and D. P. Riley, *Science*, 1999, **286**, 304–306.
9 Y. Noritake, N. Umezawa, N. Kato and T. Higuchi, *Inorg. Chem.*, 2013, **52**, 3653–3662.
10 K. Dürr, D. A. Yalalov, F. W. Heinemann, S. B. Tsogoeva and I. Ivanovic-Burmazovic, *Z. Naturforsch.*, 2010, **65b**, 258–262.
11 K. Aston, N. Rath, A. Naik, U. Slomczynska, O. F. Schall and D. P. Riley, *Inorg. Chem.*, 2001, **40**, 1779–1789.
12 M. Grau, J. England, R. Torres Martin de Rosales, H. S. Rzepa, A. J. P. White and G. J. P. Britovsek, *Inorg. Chem.*, 2013, **52**, 11867–11874.
13 D. G. Lonnon, G. E. Ball, I. Taylor, D. C. Craig and S. B. Colbran, *Inorg. Chem.*, 2009, **48**, 4863–4872.
14 G.-F. Liu, K. Dürr, R. Puchta, F. W. Heinemann, R. van Eldik and I. Ivanovic-Burmazovic, *Dalton Trans.*, 2009, 6292–6295.
15 R. A. Geiger, S. Chattopadhyay, V. W. Day and T. A. Jackson, *J. Am. Chem. Soc.*, 2010, **132**, 2821–2831.
16 A caveat needs to be added as activities determined for different catalyst systems by different groups of researchers in different labs are not always strictly comparable.
17 Y. G. Abashkin and S. K. Burt, *Inorg. Chem.*, 2005, **44**, 1425–1432.
18 X. Jiang, H. Liu, B. Zheng and J. Zhang, *Dalton Trans.*, 2009, 8714–8723.
19 In phosphate buffer (pH 9), the catalyst displays sluggish oxygen evolution activity, levelling off at 3% at a slower rate (R_0 = 18 μM min^{-1}), which may hint at a possible role of the borate buffer in the dismutation reaction see also M. E. Deary, *et al.*, *Org. Biomol. Chem.*, 2013, **11**, 309–317.
20 The exact role of imidazole is unclear at this stage, but the addition of imidazole has no effect in acetonitrile. In the absence of imidazole in aqueous solution, no oxygen evolution is observed using [Mn(**3**)(OTf)$_2$] and H_2O_2 in borate buffer at pH 9.2. Furthermore, no oxygen evolution was observed using $MnCl_2 \cdot 4H_2O$, imidazole, H_2O_2 and borate buffer at pH 9.2, but oxygen evolution commenced upon addition of [Mn(**3**)(OTf)$_2$].
21 K. Serbest, A. Özen, Y. Ünver, M. Er, I. Degirmencioglu and K. Sancak, *J. Mol. Struct.*, 2009, **922**, 1–10.
22 U. Fekl and R. van Eldik, *Eur. J. Inorg. Chem.*, 1998, 389–396.
23 C. Bull, E. C. Niederhoffer, T. Yoshida and J. A. Fee, *J. Am. Chem. Soc.*, 1991, **113**, 4069–4076.
24 Bruker AXS SHELXTL, Madison, WI; SHELX-97G. M. Sheldrick, *Acta Crystallogr. A*, 2008, **64**, 112–122, SHELX-2013, http://shelx.uni-ac.gwdg.de/SHELX/index.php.